Naval Research Laboratory

Washington, DC 20375-5320 NRL/PU/7641--00-411 June 2000

Mountain Waves in the Stratosphere

S.D. ECKERMANN
Space Science Division

D. BROUTMAN
Computational Physics, Inc.

K.A. TAN
University of New South Wales

P. PREUSSE
University of Wuppertal

J.T. BACMEISTER
Universities Space Research Association

Reprinted from *2000 NRL Review*

Report Documentation Page

Form Approved
OMB No. 0704-0188

1. REPORT DATE	2. REPORT TYPE	3. DATES COVERED
JUN 2000		**00-00-2000 to 00-00-2000**

4. TITLE AND SUBTITLE	5a. CONTRACT NUMBER
Mountain Waves in the Stratosphere	5b. GRANT NUMBER
	5c. PROGRAM ELEMENT NUMBER
6. AUTHOR(S)	5d. PROJECT NUMBER
	5e. TASK NUMBER
	5f. WORK UNIT NUMBER
7. PERFORMING ORGANIZATION NAME(S) AND ADDRESS(ES) **Naval Research Laboratory, Space Science Division,Washington,DC,20375**	8. PERFORMING ORGANIZATION REPORT NUMBER
9. SPONSORING/MONITORING AGENCY NAME(S) AND ADDRESS(ES)	10. SPONSOR/MONITOR'S ACRONYM(S)
	11. SPONSOR/MONITOR'S REPORT NUMBER(S)

12. DISTRIBUTION/AVAILABILITY STATEMENT
Approved for public release; distribution unlimited

13. SUPPLEMENTARY NOTES

14. ABSTRACT

15. SUBJECT TERMS

16. SECURITY CLASSIFICATION OF:			17. LIMITATION OF ABSTRACT	18. NUMBER OF PAGES	19a. NAME OF RESPONSIBLE PERSON
a. REPORT **unclassified**	b. ABSTRACT **unclassified**	c. THIS PAGE **unclassified**	**Same as Report (SAR)**	**16**	

Cover caption:

Mountain wave-induced polar stratospheric clouds (PSCs) in the stratosphere over Kiruna, Sweden on 25th January 2000 during the SAGE III Ozone Loss and Validation Experiment (SOLVE). The MWFM model discussed herein forecasted both the large mountain waves and the wave-induced PSCs over Kiruna on this day. MWFM forecasts also predicted little or no turbulence associated with these waves, and thus stratospheric ER-2 flights from Kiruna were feasible. Photo by Geir Braathen, Norwegian Institute for Air Research.

Mountain Waves in the Stratosphere

S.D. Eckermann
Space Science Division

D. Broutman
Computational Physics, Inc.

K.A. Tan
University of New South Wales

P. Preusse
University of Wuppertal

J.T. Bacmeister
Universities Space Research Association

This article describes recent progress in our efforts to model, forecast, and observe mountain waves in the stratosphere. We have developed a numerical model that globally forecasts stratospheric mountain wave effects. Recent improvements to that model are outlined briefly. We illustrate the potential usefulness of these model forecasts by successfully "hindcasting" some cases where unexpected severe turbulence was encountered by aircraft at stratospheric cruise altitudes. We also show the model's usefulness in forecasting mountain-wave-induced polar stratospheric clouds, which play a crucial role in stratospheric ozone depletion. Finally, we describe some recent satellite observations that have provided us with global data on stratospheric mountain wave distributions, allowing us to benchmark our global mountain wave predictions against data for the first time.

INTRODUCTION

Fluids radiate waves when disturbed by an obstacle. A familiar example is the V-shaped pattern of surface waves produced by a moving ship at sea or by a stationary rock in a stream. A related phenomenon occurs when winds blow over a mountain. The resulting oscillations in the wind and temperature profiles are known as mountain waves, and they can radiate energy over very large distances, both vertically and horizontally. Mountain waves can sometimes be identified by rows of lenticular clouds that form in the ascent (cooling) phases of the waves.

Mountain waves are important in many contexts. They can trigger intense downslope windstorms and severe clear-air turbulence, both of which pose safety hazards to aviation. Mountain waves also cause important changes to the winds, on a global as well as local scale. Yet the mountain waves themselves are too small in scale (typically 10 to 100 km horizontal wavelengths) to be resolved adequately in global numerical weather prediction (NWP) models. Hence their effects must be parameterized, and much research has been directed at improving such parameterization schemes. In models such as the Navy Operational Global Atmospheric Prediction System (NOGAPS), the inclusion of parameterized mountain-wave effects has led to more accurate forecasts.

Mountain waves can often propagate into the stratosphere (heights of ~10 to 50 km) and beyond, although far less is known about the waves at these higher altitudes. Here we summarize some recent research and forecasting work that has shed new light on high-altitude mountain waves and their influence on stratospheric processes.

THE MOUNTAIN WAVE FORECAST MODEL

Our main modeling tool is the Mountain Wave Forecast Model (MWFM). MWFM blows atmospheric winds (from NWP forecasts, for example) over digital representations of the Earth's major topographical features and calculates a spectrum of forced mountain waves. The model simulates subsequent propagation of these waves, keeping track of their amplitudes along the way. The MWFM code has been developed over the past 7 years at NRL into an operational forecasting model (MWFM 1.0)[1] that is run daily over the continental United States and on a campaign basis over other regions of the globe.

The basic MWFM 1.0 algorithm incorporates a number of simplifying assumptions. For instance, it deals exclusively with the long quasi-two-dimensional ridges that characterize many mountainous regions. These ridges tend to force plane wave patterns that are easier to model. However, many hills and mountains are more three-dimensional (3D) in nature, and tend to radiate nonplanar wave fields that sometimes resemble ship wave patterns. For example, Fig. 1(a) shows ship wave-like mountain wave patterns over Jan Mayen, a small island approximately 550 km northeast of Iceland. The wave patterns here are made visible by banded wave clouds in the troposphere associated with the ascent (cooling) and descent (warming) phases of waves. These waves originated from Mount Beerenberg , a large quasi-circular volcanic mountain that dominates the topography of Jan Mayen and above which mountain wave clouds are often observed.

We have investigated ways in which mountain wave patterns like these can be accurately yet efficiently parameterized in a global forecast model like MWFM. To study them in more depth, we have developed and used a nonlinear 3D model of atmospheric flow over topography. Results for flow over a circular bell-shaped hill are shown in Fig. 1(b). In this experiment, the wind vector rotates counterclockwise with altitude (so-called "turning flow"). We see that a skewed V-shaped mountain wave pattern is generated.

We have developed numerical ray-tracing algorithms that can accurately reproduce these 3D mountain wave fields. Figure 1(c) shows output from a formal ray-tracing algorithm that we have developed for 3D mountain wave problems,[2] applied here to an idealized turning-flow problem over a circular bell-shaped mountain. The result here agrees very well with formal numerical solutions. Peak wave amplitudes only are plotted in Fig. 1(c). Figure 1(d) shows results from a simpler ray-based algorithm, except here the synthesis incorporates both amplitude and phase. Again, the salient features of the radiated mountain wave field are captured.

Ray-based algorithms and other improvements are being built into the next-generation model, a test version of which now exists (MWFM 2.0-β). Next we discuss applications of the MWFM models to stratospheric forecasting and research problems.

TURBULENCE FORECASTS FOR STRATOSPHERIC AIRCRAFT

The NASA ER-2

NASA uses a Lockheed ER-2 aircraft in its research program. The ER-2 is similar to a U-2 military aircraft, but it is approximately 30% bigger, with a 20-ft longer wingspan to accommodate large scientific payloads (up to ~1 ton). Like the U-2, it is a long-range aircraft (~4000 km) that flies in the stratosphere at cruise altitudes of ~20 to 22 km, or ~70,000 ft, which is twice as high as commercial airliners.

While generally stable and safe, weight constraints mean that the ER-2 does not have a wing spur, which makes it structurally vulnerable to turbulence. The stratosphere, being drier and more naturally stable than the troposphere, does not produce much of the weather-related turbulence found lower down. However, severe turbulence can occur in the stratosphere. Accumulated experience from MWFM forecasts, pilot notes, and in-flight ER-2 data have revealed that breaking mountain waves are a primary source of turbulence at ER-2 cruise altitudes. Accordingly, ER-2 flight planners have used our MWFM turbulence forecasts for some years now.[1]

Figure 2 shows an example of an ER-2 turbulence encounter. Figure 2(a) shows flight paths taken on May 2, 1996 by the NASA DC-8 (flight path shown in red) and ER-2 (flight path in brown) during the Subsonic Aircraft Cloud and Contrail Effects Special Study (SUCCESS). Both flights took off from Salina, Kansas, and headed northwest toward the Rocky Mountains looking for mountain wave clouds. Note the similar flight patterns: this occurred because the ER-2 carried nadir-viewing instruments to study the wave clouds intercepted by the DC-8, as well as any effects of DC-8 exhaust on the clouds. The irregularity of the flight patterns was due to the hunt for suitable wave clouds.

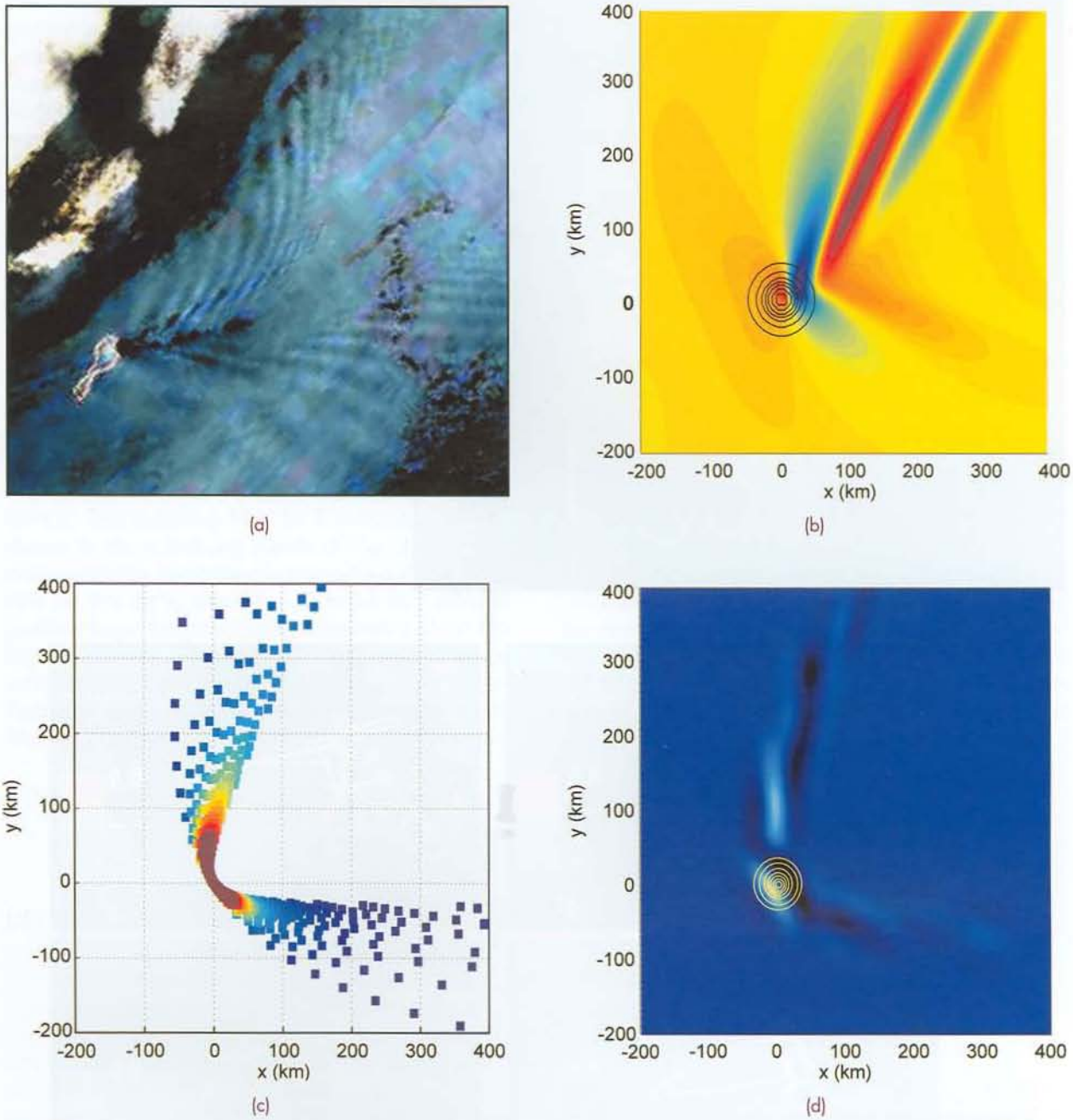

FIGURE 1
(a) Digitally enhanced false-color image of banded tropospheric clouds produced by mountain waves radiated from Jan Mayen (71.0°N, 8.5°W) on 25th January 2000 at 16:27 UT (these NOAA/AVHRR images were provided by Andreas Dörnbrack and Robert Meisner of DLR, Oberpfaffenhofen, Germany). The yellow-white bands at the top left are probably polar stratospheric cloud decks; (b) vertical displacement oscillations due to mountain waves forced by turning flow over a circular Gaussian-shaped mountain (shown with black contours, centered at $x = y = 0$), simulated with a three-dimensional atmospheric model; (c) ray-based synthesis of mountain wave vertical displacement amplitudes from turning flow over a circular mountain, with red depicting largest amplitudes and dark blue showing smallest amplitudes; (d) a simpler ray-based synthesis of the same mountain wave problem as in (c), but here incorporating both amplitude and phase.

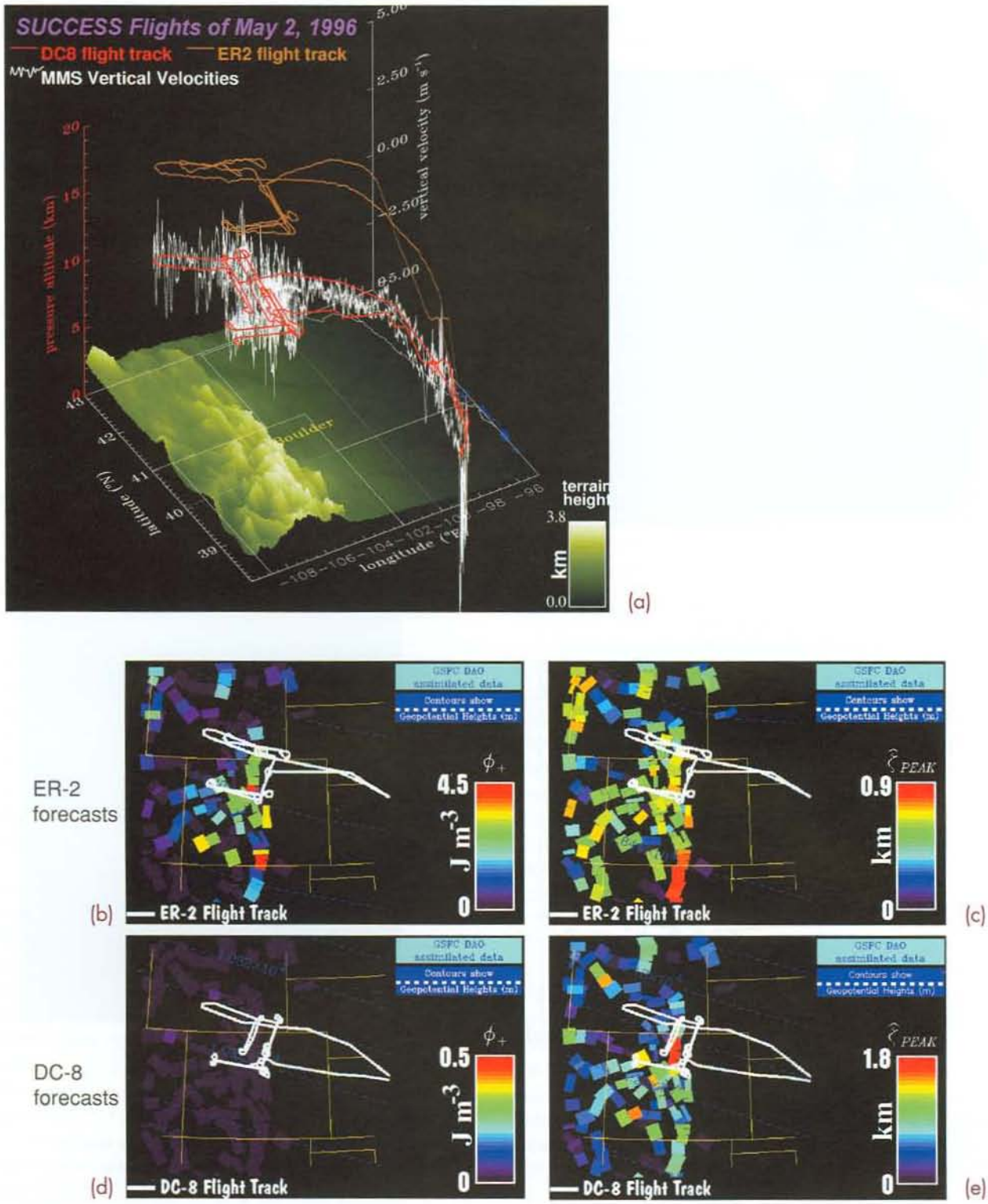

FIGURE 2
(a) Three-dimensional plot of flight paths taken on May 2, 1996 by NASA's DC-8 (red curve) and ER-2 (brown curve) research aircraft. Underlying topographic elevations are plotted in green (see color bar). Vertical velocities measured on the DC-8 are plotted along the flight track in white. (b) MWFM 1.0 turbulence forecast at 70 to 100 hPa (heights ~16-18 km, the approximate ER-2 cruise altitude here) using assimilated data for May 2, 1996 at 06:00 UT from NASA's DAO. (c) MWFM 1.0 forecast of peak vertical displacement amplitudes due to mountain waves at 70 hPa. (d) MWFM 1.0 turbulence forecast at 200 to 250 hPa (heights ~10-12 km); (e) MWFM 1.0 forecast of peak vertical displacement amplitudes at 200 hPa. In panels (b)-(e), the relevant flight track is plotted in white, the squares correspond in each case to the "ridge element" that forced this particular mountain wave, and yellow lines show state borders.

The white curve superimposed on the DC-8 flight path in Fig. 2(a) shows atmospheric vertical velocities measured onboard the DC-8. Large-amplitude oscillations are evident over the Rockies, which were later analyzed and shown to be mountain waves.[3] Despite the large wave activity, the DC-8 pilot reported no unusual in-flight turbulence. On the ER-2, no vertical velocity measurements were made, although wave oscillations were evident in the routine navigational wind data. The ER-2 pilot reported "heavy turbulence" at cruise altitudes and classified the flight afterwards as "highly turbulent". Interestingly, MWFM turbulence forecasts were made available during SUCCESS, but they do not appear to have been utilized, apparently because tropospheric clouds and contrails were the primary focus of the mission. Thus, it is interesting to reanalyze the May 2, 1996 situation using MWFM.

Since the NWP forecast data are no longer available, we use analyzed winds and temperatures for that day from NASA's Data Assimilation Office (DAO). The resulting MWFM 1.0 "hindcasts" are shown in the remaining panels of Fig. 2. At DC-8 cruise altitudes (atmospheric pressures ~190 to 240 hPa for this flight, altitudes ~10 to 11 km), MWFM predicts large mountain wave amplitudes along the flight track (Fig. 2(e)) but essentially no wave-induced turbulence (Fig. 2(d)). This is consistent with the in-flight data. Conversely, MWFM hindcasts at ER-2 altitudes (pressures ~60 to 80 hPa on this flight) show moderate wave activity (Fig. 2(c)) and fairly intense wave-induced turbulence (Fig. 2(b)). Experience with MWFM forecasts has shown that a useful working threshold for "uncomfortable" stratospheric turbulence is a value ~1 J m^{-3}. Many values in Fig. 2(b) along the ER-2 flight track are well in excess of this, with a peak value of 6.4 J m^{-3} forecast 6 hours earlier (not shown). Again, these features are entirely consistent with the navigational data and pilot notes from this flight.

Figure 3 shows the turbulence hindcast from the MWFM 2.0-β model, which has interesting similarities and differences to the MWFM 1.0 forecast (Fig. 2(b)). While the activity here is more limited, both in absolute magnitude and geographical coverage, intense turbulence occurs here also at the lower corner of the U-shaped ER-2 flight pattern. A significant portion of this ER-2 flight occurred in this region, with four separate flight segments passing through the hindcasted turbulent region. Again, this hindcast is consistent with the available data from this flight.

Alaska Airlines Flight 67

Forecasts like these may also have applications for existing commercial fleets. Though they fly considerably lower than the ER-2, these aircraft can also encounter severe unforecast turbulence in the lowermost regions of the stratosphere, often with serious consequences for passengers and crew.

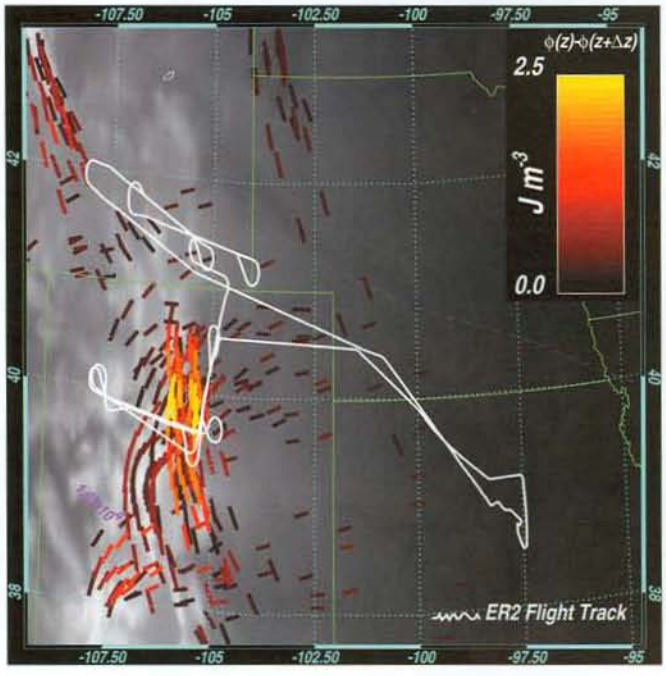

FIGURE 3
MWFM 2.0-β forecast of mountain-wave-induced turbulence at 70 to 100 hPa on May 2, 1996 at 12:00 UT, using DAO assimilated data of 2.5° × 2° grid resolution (see dotted blue grid). The ER-2 flight track on this day is plotted in white, state borders are plotted in green. The line color corresponds to the intensity of wave-induced turbulence, while its alignment corresponds to the orientation of wave phase fronts (see Fig. 1), as provided by the newly implemented ray-tracing algorithms. The underlying gray scale shows topographic elevations.

We illustrate this by using MWFM 2.0-β to investigate an unexplained encounter with severe turbulence by an Alaska Airlines Boeing 737 aircraft. The National Transportation Safety Board (NTSB) report of this incident makes compelling reading: only the salient details are summarized below. The flight took off from Juneau, Alaska, at 6:10 p.m. on December 22, 1996, and headed for Anchorage at a cruise altitude of 35,000 ft. In-flight turbulence was light until it flew over Mount Fairweather, whereupon turbulence immediately became moderate. Severe clear-air turbulence occurred roughly 30 miles east of Yakutat, Alaska, a region marked with the green diamond in Fig. 4. All three flight attendants were injured, two seriously (one attendant suffered a fractured pelvis and elbow, the other a fractured vertebrae in her back). The seriously injured attendants were at the back of the plane, preparing the drinks cart, when they were thrown violently into the ceiling and then onto the cabin floor by "two massive jolts."

SIGMET (significant meteorological information) advisories indicated no turbulence in this region; however, these advisories did not account for mountain waves. Figure 4 shows results of an MWFM 2.0-β hindcast for the region using National Center for Environmental Prediction (NCEP) reanalysis data for December 23, 1996 at 00:00 UT. We see a zone of mountain-wave-induced turbulence predicted between Mount Fairweather and the estimated location of the incident. Given our criterion for "uncomfortable" turbulence of ~1 J m^{-3}, the values of ~2 to 4.5 J m^{-3} in this region are consistent with the moderate-to-severe turbulence encountered along this flight segment. Interestingly, turbulence was almost entirely absent in the MWFM postcast at the next level down (250 to 300 hPa: ~28,000 to 33,000 ft). Thus, if these forecasts had been available at the time, a simple reroute to a slightly lower flight altitude may have avoided this incident.

At present, we provide daily MWFM forecasts of mountain wave amplitudes in the lower atmosphere over the continental United States <http://uap-www.nrl.navy.mil/dynamics/html/mwfmforecasts.html>, mainly in response to repeated requests from the gliding community. The above examples indicate that our upper-level turbulence forecasts have important potential applications not just for the ER-2 and other high-altitude aircraft, but also for commercial and military aviation. Other operational stratospheric aircraft include the M-55 Geophysica, the Grob 520T Egrett, the SR-71 Blackbird, and many jet fighter aircraft, like the Navy F-15 jet fighters and the Russian MiG-25. Furthermore, NASA and the aerospace industry are developing technologies for next-generation high-altitude research aircraft, through the APEX and ERAST programs, and for a supersonic passenger aircraft that would fly at or just below typical ER-2 altitudes (i.e., well into the stratosphere). Global forecasts of mountain-wave-induced stratospheric turbulence would clearly be desirable to ensure

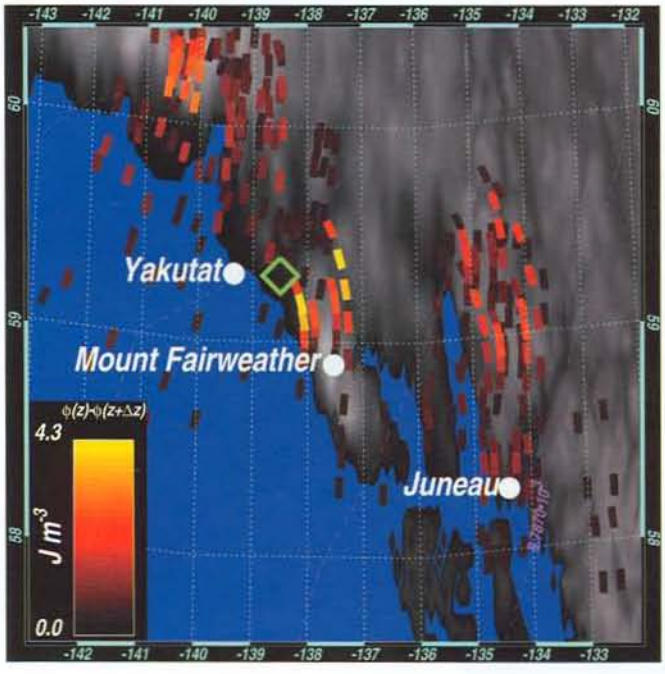

FIGURE 4
MWFM 2.0-β hindcast of mountain-wave-induced turbulence at 200 to 250 hPa (~33,000-38,000 ft) on December 23, 1996 at 00:00 UT, using NCEP reanalysis data of 1° × 1° grid resolution (see dotted blue grid). The green diamond shows the approximate estimated location of a severe turbulence encounter by Alaska Airlines Flight 67 at ~35,000 ft at 7:12 pm local time on December 22.

smooth, safe flight routes for such aircraft. How these forecasts could be rapidly and accurately communicated for in-flight applications remains to be explored.

POLAR STRATOSPHERIC CLOUDS AND OZONE DEPLETION

Polar ozone is destroyed when stratospheric temperatures become very cold and polar stratospheric clouds (PSCs) form. PSC-related chemistry denitrifies the stratosphere and activates chlorine into efficient ozone-destroying forms. PSCs made of nitric acid trihydrate (NAT) form at stratospheric temperatures below T_{NAT} ~ 195 K (–109 °F), while ice PSCs form below the frost point temperature T_{ICE} ~188 K (–121 °F). Thus, forecasting ozone depletion requires accurate forecasts of the temperature drops that lead to PSC formation.

On November 30, 1999, stratospheric ozone levels over the United Kingdom, Belgium, the Netherlands, and Scandinavia plummeted to Antarctic-like lows, prompting a press release from the European Space Agency. That same day, NASA's DC-8 flew to Kiruna, Sweden, to commence Phase 1 of the SAGE III Ozone Loss and Validation Experiment (SOLVE). As it circled to land, PSCs were observed visually from the aircraft well to the south of Kiruna (Fig. 5(b)). The following day, spectacular banded PSCs were visible from the ground in Oslo, Norway (Fig. 5(c)). On November 30, the POAM science team in Code 7227 reported PSC detections over Scandinavia (see Fig. 5(a)) using NRL's POAM instrument, which routinely detects Arctic PSCs from space.[4]

In recent years, we have used MWFM to predict and research mountain-wave-induced PSCs over Scandinavia in support of airborne PSC measurements made during winter by European research teams.[5-7] During SOLVE, as well as mountain-wave turbulence forecasting, we provided daily MWFM forecasts to help direct NASA's DC-8 and ER-2 aircraft toward possible encounters with nonturbulent mountain-wave-induced PSCs.

November 30, 1999 was one of the first days when MWFM forecasts were supplied operationally for SOLVE. MWFM 2.0-β predictions based on 18-hour NOGAPS forecasts for this day are shown in Fig. 5(a). Color-coded lines show peak mountain-wave temperature amplitudes at 30 hPa (an altitude of ~24 km). These plots are similar to the wave amplitude plots in Fig. 1(c): here, too, we see V-shaped wave patterns forecast west of Oslo. The NOGAPS forecast data are made available to us year-round by Dr. Timothy Hogan of Code 7500 at NRL, Monterey.

Mean stratospheric temperatures are plotted with blue dashed contours in Fig. 5(a). A broad region with temperatures below 192 K was forecast by NOGAPS over northern Britain, southern Scandinavia, and regions of northern Europe. Thus, NAT PSCs can form here and deplete ozone, possibly accounting for the reduced ozone levels reported over this region (although a regional ascending circulation may also be implicated[8,9]). Forecasts a few days later gave significantly warmer temperatures, consistent with the return of more normal observed ozone levels a day or so later.

NAT PSCs, however, are generally hazy and hard to see from the ground. Conversely, the PSCs photographed in Figs. 5(b) and 5(c) are quite opaque. They are clearly visible from a long way away, and so are more likely to have been ice PSCs. However, ice formation at these altitudes requires temperatures below 188 K, which were not forecast by NOGAPS or other NWP models.

The MWFM forecasts appear to explain the ice PSCs over southern Scandinavia. In Fig. 5(a), stratospheric mountain waves are forecast west of Oslo, with peak amplitudes in the ~4 to 8 K range. This provides additional cooling that drops temperatures below the frost point in the cooling (ascent) phase of the wave, thereby triggering ice formation. Indeed, like the low-level clouds in Fig. 1(a), the PSCs in Fig. 5(c) show the "banding" that is characteristic of clouds formed in the various cooling (ascent) phases of a mountain wave. Other observations and MWFM results have revealed that mountain-wave-induced PSCs commonly form over northern Scandinavia and other mountainous Arctic regions during winter.[5,6] The combined effects of wave-induced PSC formation over the entire Arctic may result in an overall reduction in stratospheric ozone levels.[7]

The reduced ozone and spectacular PSC displays over Europe on November 30 were unusual and somewhat troubling; these processes are usually confined to less-inhabited polar regions. Nonetheless, the basic features of this event appear to have been forecast in Fig. 5(a), indicating that model forecasts of this kind might be useful for low ozone alerts over populated mountainous regions. At the time of writing, these and other MWFM forecasts are being generated daily at NRL and made available to in-field science teams during SOLVE throughout the Arctic winter of 1999-2000.

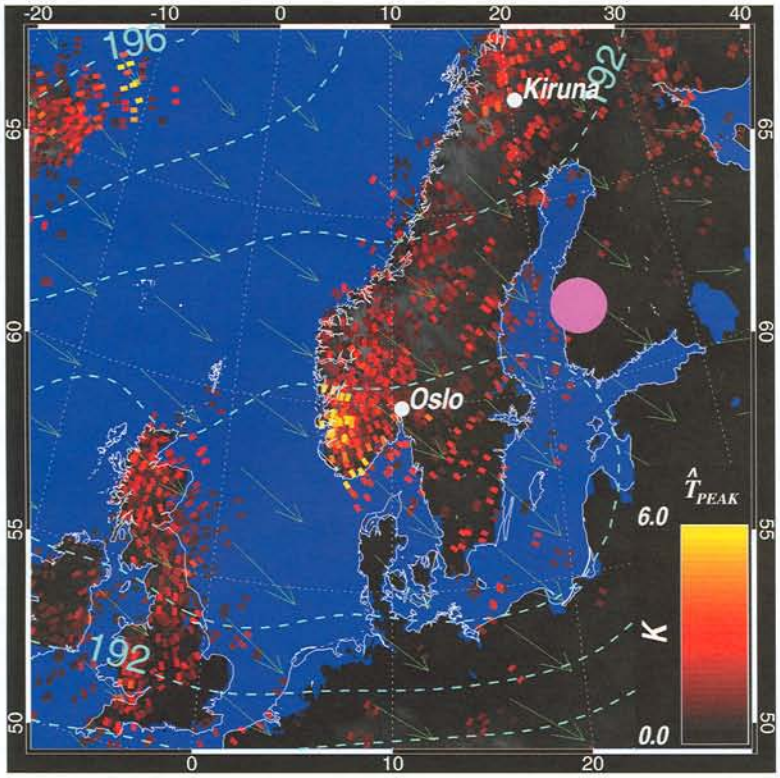

(a)

(b)

(c)

FIGURE 5
(a) 18-h MWFM 2.0-β forecasts of stratospheric mountain waves at 30 hPa on November 30, 1999, using NOGAPS forecast output. Dashed blue contours show mean temperatures, red-yellow bars show ray-based forecasts of peak mountain wave temperature amplitudes. The pink spot shows the ground-level location of the POAM III PSC detection on this day. Blue arrows indicate wind direction. (b) Photograph from the DC-8 by Dr. Mark Schoeberl, NASA Goddard Space Flight Center, on November 30, 1999. Cirrus-like PSCs are visible in the distance above the DC-8 wingtip. (c) Photograph by Geir Braathen, Norwegian Institute for Air Research, of iridescent red PSCs over southern Norway at dusk on December 1, 1999.

GLOBAL MOUNTAIN WAVE MEASUREMENTS FROM SPACE

Previous sections have shown how regional stratospheric data help in assessing and refining MWFM stratospheric forecasts. MWFM can also provide global forecasts, which are useful for studies of global PSC formation[5,6] and associated ozone depletion,[7] as well as global circulation patterns produced by mountain wave drag. Unfortunately, no global measurements have been made of stratospheric mountain waves to allow similar observational assessments of these global forecasts. This is because, like global NWP and climate models, the global data provided by satellite instruments have been too coarse spatially to resolve mountain waves.

On November 3, 1994, the Space Shuttle Atlantis took off from Cape Canaveral with CRISTA-SPAS (a Shuttle pallet satellite) in the payload. This recoverable satellite experiment carried two atmospheric measuring instruments: the University of Wuppertal's Cryogenic Infrared Spectrometers and Telescopes for the Atmosphere (CRISTA) and Code 7640's Middle Atmosphere High Resolution Spectrograph Investigation (MAHRSI). The CRISTA instrument was cryogenically cooled to liquid helium temperatures and acquired data using three telescopes and four infrared spectrometers. This allowed CRISTA to acquire some of the highest spatial resolution stratospheric data to date from a space-based platform. Still, until recently, it was unclear whether even these measurements had adequate resolution to detect mountain waves. Many years of careful modeling and data analysis have finally answered this question definitively: CRISTA did measure stratospheric mountain waves.[10]

As summarized in Fig. 6, one of the clearest mountain wave detections by CRISTA occurred over the southern tip of South America. During deployment of CRISTA-SPAS from the shuttle on November 4, the astronauts took a series of photographs: one of them is shown in Fig. 6(b). As shown in Fig. 6(a), the Shuttle was orbiting northwestward over the east coast of South America at the time, and the photo in Fig. 6(b) looks northwestward across the southern Andes. It shows a broad linear cloud band running north-south along the Andes, and banded wave clouds downstream of this region. This suggests that mountain waves were being generated in the lower atmosphere by flow across the Andes at the time CRISTA-SPAS was deployed.

Two days later, CRISTA-SPAS was in free orbit (~20 to 100 km behind the Shuttle) and CRISTA was acquiring stratospheric data. At ~06:24 UT on November 6, CRISTA took three successive stratospheric temperature measurements over South America, at the locations labeled 1, 2, and 3 in Fig. 6(a). Vertical profiles of temperature fluctuations extracted from those measurements are plotted in Fig. 6(c). All three show similar wavelike temperature oscillations in the stratosphere from 15 to 30 km, with a vertical wavelength λ_z ~ 6 to 7 km and peak temperature amplitudes $\hat{T}$ of ~ 3 to 7 K.

MWFM hindcasts predicted intense stratospheric mountain wave activity at this particular time and location.[10] The remaining panels in Fig. 6 show results of a model simulation of atmospheric flow across the Andes, using a two-dimensional version of the nonlinear regional model used in Fig. 1(b).[11] This model experiment used actual background winds and temperatures at the time of these particular CRISTA measurements, as well as realistic Andean topography (Fig. 6(d)). Figure 6(e) shows the resulting stratospheric temperature response, with mountain waves penetrating into the uppermost regions of the stratosphere and temperature amplitudes of ~4 to 8 K. The potential temperature surfaces in Fig. 6(e), which remain flat in the absence of waves, begin to fold and overturn near 30 km, indicating that these mountain waves are breaking and generating intense turbulence. Figure 6(f) compares a model vertical profile at x = 650 km with the CRISTA data from measurement location 1. The amplitude, phase, and vertical wavelength of the two oscillations are quite similar. These and other tests[10,11] prove beyond doubt that the fluctuations in the CRISTA data in Fig. 6(c) are stratospheric mountain waves that emanated from the southern Andes.

CRISTA took measurements like these over the entire globe during the week-long mission. The results in Fig. 6 suggest that these CRISTA data can provide global information on stratospheric mountain waves. Figure 7(a) shows peak amplitudes of temperature perturbations ($\hat{T}$, see Fig. 6(b)) estimated from all CRISTA stratospheric temperature measurements in the Northern Hemisphere on November 9, 1994, at a height of 25 km. Most noticeable is a region of enhanced oscillation amplitudes over a mountainous region of central Eurasia, which takes in the Sayan Ranges, Altay Mountains, and Tian Shan (Fig. 7(b)). An MWFM 2.0-β hindcast for November 9 at z = 25 km is shown in Fig. 7(c). The hindcast reproduces this region of enhanced stratospheric mountain wave activity. Interestingly, the hindcast shows little or no mountain wave activity over other mountainous regions, such as western North America, in agreement with the observations.

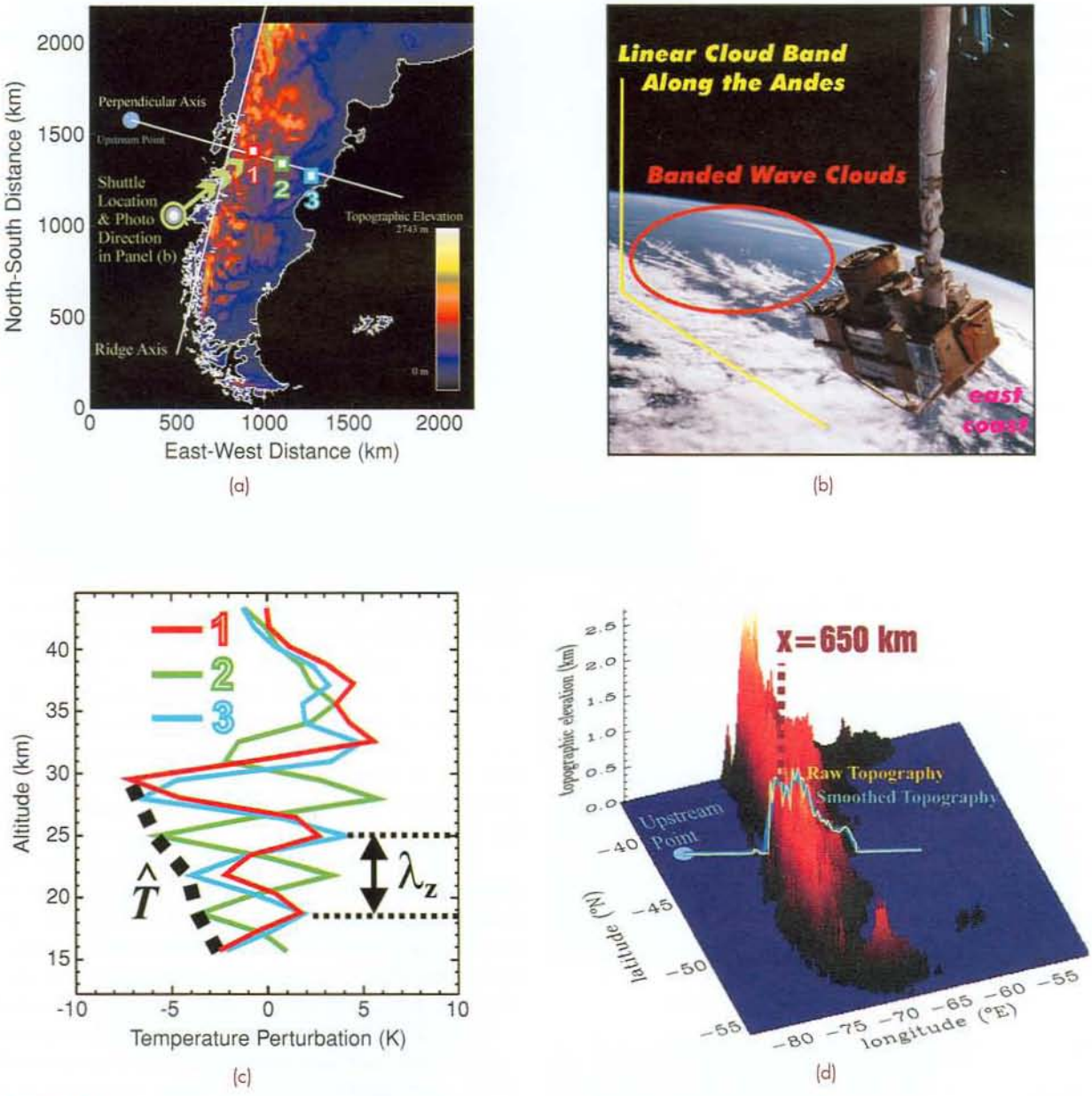

FIGURE 6

(a) Topographic elevations for southern South America (linear color scale). (b) Astronaut photograph over southern South America showing deployment of CRISTA-SPAS from Atlantis, November 4, 1994, 12:18 UT. The nadir point and orbital motion of the Shuttle at this time are shown with a circle and arrow, respectively, in panel (a). The cylindrical assembly on the satellite houses CRISTA. The east coast of Argentina and Atlantic Ocean are visible to the right, banded mountain wave clouds downstream of the Andes are visible to left of CRISTA-SPAS. (c) Vertical profiles of temperature perturbations from three successive CRISTA scans on November 6, 1994 at ~06:24 UT, acquired from locations 1, 2, and 3 shown in panel (a). (d) Three-dimensional topographic elevations, including a section perpendicular to the Andean ridge axis used for two-dimensional model simulations, results of which are shown in panel (e).

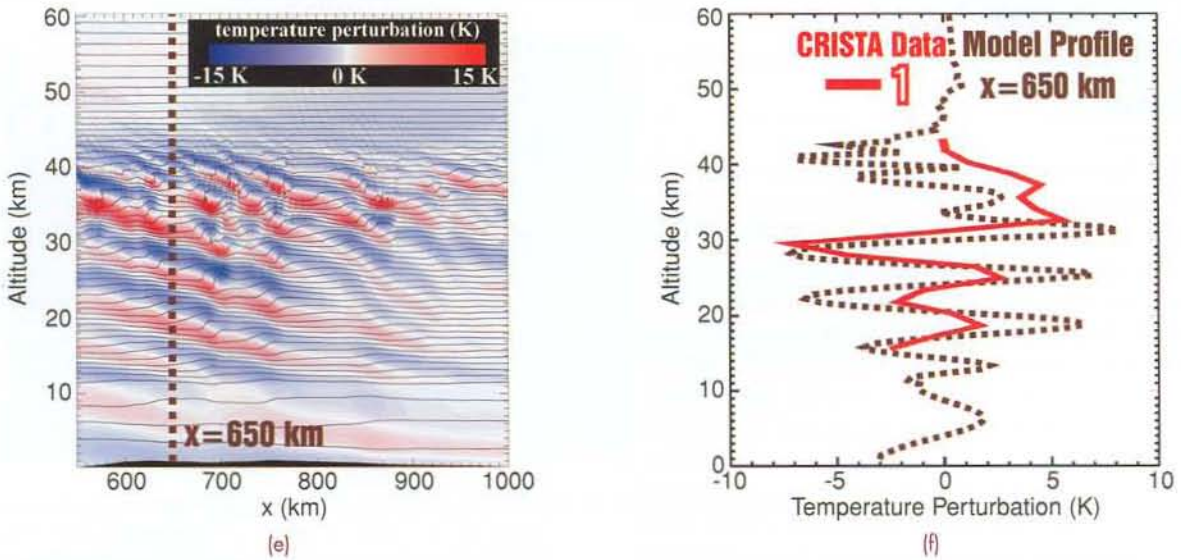

FIGURE 6 (continued)
(e) Model-generated temperature variability in the troposphere and stratosphere on November 6, 1994 due to flow over the smoothed topography in panel (d). Contours show potential temperature surfaces (essentially, material surfaces), with constant logarithmic separation between adjacent contours. Colors show temperature perturbations (color-scale given top-right); (f) Dotted brown curve shows a vertical profile of simulated temperature perturbations at x = 650 km, 10 hours into the model simulation. Red curve shows CRISTA data from location 1, shown also in panel (c).

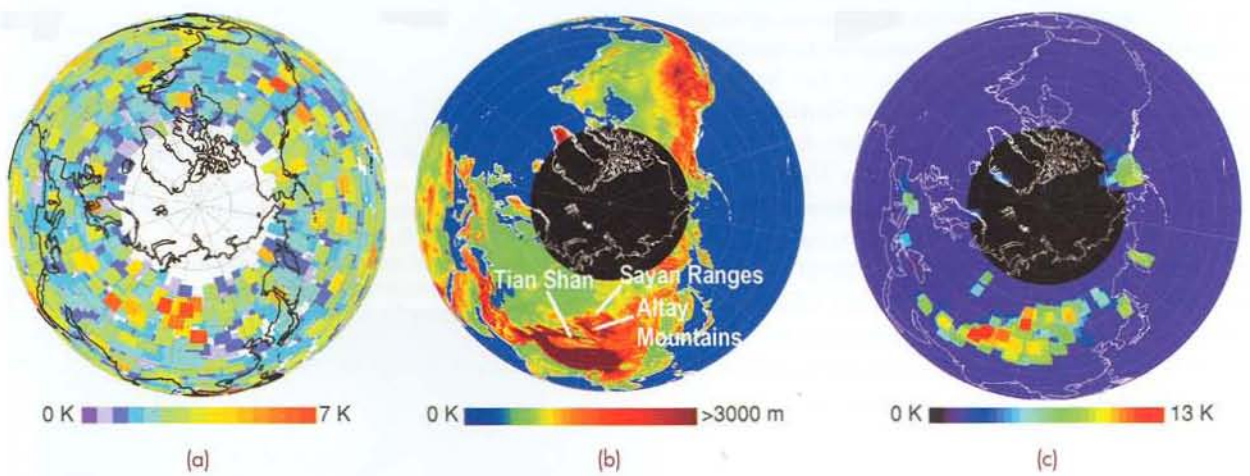

FIGURE 7
(a) Polar orthographic maps of amplitudes $\hat{T}$ from CRISTA temperature profiles taken over the Northern Hemisphere on November 9, 1994 at z = 25 km; (b) topographic elevations in the Northern Hemisphere; (c) MWFM 2.0-β hindcasts of amplitudes $\hat{T}$ at 25 km, using DAO assimilated winds and temperatures at 12:00 UT on this date. Modeled waves with λ_z < 5 km were not plotted since CRISTA is not sensitive to them. Pixels in (a) and (c) are plotted in order of ascending amplitude and are sized to maximize coverage while minimizing pixel overlap. These plots are adapted from Ref. 10.

These results show that advances in remote sounding satellite technology can now provide global data on mountain waves in the stratosphere. Such data offer the prospect of improved observational assessments of global MWFM forecasts.

SUMMARY

We have summarized ongoing work in the Upper Atmospheric Physics Branch (Code 7640) related to stratospheric mountain waves. Theoretical and algorithmic developments are being used to improve the NRL Mountain Wave Forecast Model (MWFM). Regional data from aircraft campaigns have proved particularly valuable in assessing the performance of both older and newer versions of the model. Data from the latest satellite instruments can now be used to extract information on stratospheric mountain waves, permitting observational assessments of MWFM's global forecasting capabilities. Other areas where improvements can be made in the model have been identified and targeted for future research.

We have used MWFM to investigate some of the important effects that mountain waves exert on the dynamics, chemistry, and cloud physics of the stratosphere. We have shown how mountain waves produce severe stratospheric turbulence, which poses a safety hazard to stratospheric aircraft, as well as polar stratospheric clouds, which deplete ozone. MWFM now forecasts these phenomena. This recent modeling and forecasting work has interfaced synergistically with several other NRL research projects, such as satellite measurements made by the Space Science Division (Code 7600) and the Remote Sensing Division (7200) and global forecasts issued by the Marine Meteorology Division (Code 7500).

When compared with the extensive literature on mountain waves in the lower atmosphere, we have probably only scratched the surface in uncovering and understanding mountain wave effects in the stratosphere. Parallel improvements in models and observations offer exciting prospects for future discoveries and improved knowledge and modeling capability.

[Sponsored by ONR and NASA]

REFERENCES

[1] J.T. Bacmeister, P.A. Newman, B.L. Gary, and K.R. Chan, "An Algorithm for Forecasting Mountain Wave-Related Turbulence in the Stratosphere," *Weather Forecast.* **9**, 241-253 (1994).

[2] D. Broutman, J.W. Rottman, and S.D. Eckermann, "A Hybrid Method for Wave Propagation from a Localized Source, with Application to Mountain Waves," *Q.J.R. Meteorol. Soc.*, submitted (2000).

[3] J. Dean-Day, K.R. Chan, S.W. Bowen, T.P. Bui, B.L. Gary, and M.J. Mahoney, "Dynamics of Rocky Mountain Lee Waves Observed During SUCCESS," *Geophys. Res. Lett.* **25**, 1351-1354 (1998).

[4] M.D. Fromm, R.M. Bevilacqua, J. Hornstein, E. Shettle, K. Hoppel, and J.D. Lumpe, "An Analysis of Polar Ozone and Aerosol Measurement (POAM) II Arctic Polar Stratospheric Cloud Observations, 1993-1996," *J. Geophys. Res.* **104**, 24,341-24,357 (1999).

[5] K.S. Carslaw, M. Wirth, A. Tsias, B.P. Luo, A. Dörnbrack, M. Leutbecher, H. Volkert, W. Renger, J.T. Bacmeister, and T. Peter, "Particle Microphysics and Chemistry in Remotely Observed Mountain Polar Stratospheric Clouds," *J. Geophys. Res.* **103**, 5785-5796 (1998).

[6] K.S. Carslaw, T. Peter, J.T. Bacmeister, and S.D. Eckermann, "Widespread Solid Particle Formation by Mountain Waves in the Arctic Stratosphere," *J. Geophys. Res.* **104**, 1827-1836 (1999).

[7] K.S. Carslaw, M. Wirth, A. Tsias, B.P. Luo, A. Dörnbrack, M. Leutbecher, H. Volkert, W. Renger, J.T. Bacmeister, E. Reimer, and T. Peter, "Increased Stratospheric Ozone Depletion Due to Mountain-induced Atmospheric Waves," *Nature* **391**, 675-678 (1998).

[8] K.B. Petzoldt, B. Naujokat, and K. Neugebohren, "Correlation Between Stratospheric Temperature, Total Ozone and Tropospheric Weather Systems," *Geophys. Res. Lett.* **21**, 1203-1206 (1994).

[9] Å. Rabbe and S.H.H. Larsen, "On the Low Ozone Values Over Scandinavia During the Winter of 1991-1992," *J. Atmos. Terr. Phys.* **57**, 367-373 (1995).

[10] S.D. Eckermann and P. Preusse, "Global Measurements of Stratospheric Mountain Waves from Space," *Science* **286**, 1534-1537 (1999).

[11] K.A. Tan and S.D. Eckermann, "Numerical Model Simulations of Mountain Waves in the Middle Atmosphere over the Southern Andes," in *Atmospheric Science Across the Stratopause*, AGU Monograph Series, D.E. Siskind, M.E. Summers, and S.D. Eckermann, editors, in press (2000).

THE AUTHORS

STEPHEN D. ECKERMANN grew up in Adelaide, Australia, and studied at the University of Adelaide, receiving an Honours degree in physics in 1986 and a Ph. D. degree in physics in 1990. As a postdoctoral research scientist, he worked at the Clarendon Laboratories at Oxford University, England, from 1990-1992, and at the Department of Physics and Mathematical Physics at the University of Adelaide from 1992-1994. In 1994 he joined Computational Physics, Inc., in Fairfax, Virginia, and began working on atmospheric research problems in collaboration with NRL scientists in the Upper Atmospheric Physics Branch. He joined NRL as a full-time employee in 1998. Dr. Eckermann's primary research interests are the modeling and forecasting of atmospheric dynamics, particularly atmospheric gravity waves.

DAVE BROUTMAN is a graduate of the University of California Los Angeles (B.A. degree in meteorology) and of Scripps Institution of Oceanography (Ph.D.). He completed postdoctoral fellowships at Cambridge University, England, and at the University of Melbourne, Australia, before joining the faculty of the University of New South Wales (applied mathematics) in Sydney, Australia. In 1998, Dave joined Computational Physics, Inc., as a research scientist and has been working closely with members of the Upper Atmospheric Physics Branch at NRL in research problems in atmospheric dynamics. His research interests include stratified fluids, gravity waves, and ocean waves.

KWOK AUN TAN received a B.S. degree in applied mathematics in 1995 from the University of New South Wales, Sydney, Australia. His primary interests are numerical techniques for high-performance computing and geophysical fluid dynamics. He was a long-term visitor to NRL DC in 1999, and worked closely with scientists in the Upper Atmospheric Physics Branch on mountain wave research problems. He is currently completing his Ph.D. dissertation at the University of New South Wales.

PETER PREUSSE joined the Physics Department at the University of Wuppertal in 1993 and works in the CRISTA science team under the leadership of Professors Dirk Offermann and Klaus Grossmann. He worked extensively on calibration hardware for the CRISTA instrument, and published his diploma thesis in 1995 on radiance calibration from CRISTA. Since 1995, his graduate work has focused on improving the retrieval software for CRISTA, and he is now in charge of the temperature and ozone retrieval work. Since 1997 he has also worked on extracting and studying gravity wave signatures in temperature and ozone data from CRISTA.

JULIO T. BACMEISTER worked in the Upper Atmospheric Research Branch at NRL from 1992 to 1998. His research interest in mountain waves began in graduate school, where he worked on simulations of downslope windstorms (also known as foehns or chinooks) as part of his Ph.D thesis. He became interested in forecasting turbulence for aircraft as a result of involvement with several NASA Polar Ozone research campaigns that used the ER-2 airplane to probe the stratosphere. Since 1998, he has worked at NASA's Seasonal-to-Interannual Prediction Project at the Goddard Space Flight Center in Greenbelt, Maryland. His current research involves climate simulation with coupled atmospheric and oceanic general circulation models.